Catalysis Today 145 (2009) 195–203

Contents lists available at ScienceDirect

Catalysis Today

journal homepage: www.elsevier.com/locate/cattod

Insights into the formation of microporous materials by *in situ* X-ray scattering techniques

Gopinathan Sankar [a,*], Wim Bras [b,*]

[a] Department of Chemistry, University College London, 20 Gordon Street, London WC1H 0AJ, UK
[b] Netherlands Organisation for Scientific Research (NWO), DUBBLE@ESRF, BP 220 F38043 Grenoble Cedex, France

ARTICLE INFO

Keywords:
Microporous materials
In situ
X-ray scattering
Catalytic materials

ABSTRACT

Here we demonstrate the power of *in situ* scattering techniques in the understanding of formation of nanoporous aluminosilicate and aluminophosphate materials. We utilised a number of X-ray techniques, in particular, *in situ* energy dispersive X-ray diffraction (EDXRD) and small angle and wide angle X-ray scattering (SAXS/WAXS) techniques for this purpose. The *in situ* SAXS measurements show the formation of homogeneous precursors in the size of *ca.* 10 nm, prior to the crystallization of LTA. The crystal size is estimated by fitting the SAXS patterns with an equation for a cubic particle, and it is revealed that the final crystal size of the LTA depends on the synthesis temperature. Whereas, the crystallisation of CoAlPO-5, occurs through the formation of poly-dispersed particles with an average size of the precursor particle of *ca.* 50 nm. Also shown the effect of temperature and structure directing organic cations on the production of CoAlPO-5 materials.

1. Introduction

X-ray scattering techniques: X-ray scattering and absorption spectroscopic techniques have been widely used in structural studies of catalytic materials [1,2]. The use of the intense X-ray beams that synchrotron radiation sources can provide has enabled many experiments over the last years to be carried out in a time-resolved mode. For structural studies the time domain of about 0.1–60 s per time frame is relevant in most cases and scattering beam lines on SR sources can easily access this time domain. Since the introduction of time-resolved combined techniques using X-ray absorption spectroscopy (XAS or QuEXAFS) and X-ray diffraction (XRD), which includes angular resolved and energy dispersive X-ray diffraction (EDXRD), several articles and reviews appeared in the literature, in particular for the study of catalytic materials under operating conditions [3–9]. Similarly, although time-resolved small angle X-ray scattering (SAXS) and in combination with wide angle X-ray Scattering (WAXS) technique has evolved over the years [10,11], very limited number of reviews have been documented [12–14] and here we review the use of the combined SAXS/WAXS technique in the field of catalysis in particular in the area of study of catalyst preparation.

At first sight it might not be clear what a technique like SAXS, which quintessentially provides large length scale information, might contribute to the study of catalysis where the local environment of catalytic sites is of pre-eminent importance. The answer to this lies in the fact that in manufacturing successful catalysts there are several stages in which these longer length scales play a role. Among features that can be studied by SAXS are the formation of the porous materials traditionally used as catalyst carriers and also the formation of metallic nano-particles with catalytic properties.

The importance of the role of WAXS, powder diffraction or EDXRD, which are ultimately all providing information on the same length scale albeit maybe not with the same angular accuracy, is rather self evident for the studies of catalysis. The combination of the information that SAXS in conjunction with powder diffraction like techniques can provide in a time-resolved experiment, however, has been recognised but still is not widely used even though the feasibility was shown a long time ago in studies of the formation of zeolitic materials under hydrothermal conditions [14,15]. The reason for this is probably due to two factors. In the first place the number of SR beam-lines that offer the possibility to combine techniques is still rather limited. The second reason is that the design of a combined experiment is more complicate then independent experiments especially when it comes down to the required sample environments. The third reason is the unavoidable fact that when one is combining techniques at least one of the experimental data sets obtained will have sub-optimal data quality. The latter fact does not imply that these data sets are useless but only that one carefully has to weigh the benefits that a combined data set can bring with respect to the optimised data sets obtained from independently carried out techniques.

* Corresponding author. Tel.: +44 207 679 0074.
E-mail address: g.sankar@ucl.ac.uk (G. Sankar).

0920-5861/$ – see front matter © 2009 Elsevier B.V.. All rights reserved.
doi:10.1016/j.cattod.2009.05.010

Technique combinations can be beneficial in certain circumstances. The first we mention here is when it is relevant to know when exactly, and in which order, structural changes on hierarchical length scales take place. The second is when it is for instance difficult to replicate the exact time profile for the parameter used to perturb the sample between independent experiments either due to the speed with which the events occur. The third reason we mention here is the possibility that a sample is not completely homogenous.

In this context we should remark that there are several other, non-X-ray based, techniques for which similar complications can occur. X-ray scattering experiments have been combined with Raman scattering, Fourier Transform Infrared Spectroscopy, Differential Scanning Calorimetry, UV–vis spectroscopy and several others [16–18].

In order to be able to judge if technique combinations are sensible one should in the first place be aware of the information that a technique can provide but also have a sound knowledge of the limitations of these techniques. An exhaustive review of this is beyond the scope of this manuscript but if we compare for instance powder diffraction, EDXRD and WAXS, i.e. techniques that provide crystallographic information, we see that there are subtle advantages and draw backs for each technique. In a conventional powder diffraction experiment one can obtain very accurate structural information but due to the angular scanning nature of this technique it is less useful for faster time-resolved experiments. However, when using a position sensitive detector one can obtain less high quality data but one has the benefit that time-resolved experiments are well feasible down to the 0.1 s/frame level. The use of such a position sensitive detector requires a fairly large X-ray transparent window in the sample environment, which can introduce temperature gradients. In such a case one can use EDXRD, in which the detector is placed under a fixed angle but where we use a non-monochromatic beam, which is detected in an energy dispersive mode. The main drawbacks of this are a further loss of angular resolution of the diffraction peaks and a higher radiation level to which the sample is exposed. This might inflict radiation damage or interfere with the chemical processes under consideration. All three techniques provide similar information but there are certain nuances in the information content of which one has to be aware to avoid over-interpretation of the results.

SAXS is a much less commonly applied technique and for many researchers in the catalysis field the information that can be derived from these experiments is less well known [16,19]. The low angle scattering intensity finds its origin in electron density variations over larger length scales. This electron density contrast can have various sources like for instance crystalline particles embedded in an amorphous matrix [20] but also long-range density fluctuations [21]. Which details exactly can be derived from a SAXS experiment depends to some degree on the specific beam-line and the detectors in use. The collimation of the beam line determines how small a scattering vector can still be resolved and therefore which size of structures one can still observe. In general, for a conventional experiment in the transmission geometry the low angle information is limited to structural dimensions of about 100–200 nm. Many beam-lines can actually observe even larger length scales but this information is concentrated in a rather limited number of detector pixels close to the intrinsic parasitic scatter cone, which is instrument dependent. It will be clear that when the scattering regime ranging from 500 to 100 nm is mapped upon three detector pixels that the factual structural information is rather limited. This limitation can be overcome by using a so-called Bonse–Hart SAXS camera but this has as a drawback that it is again a scanning technique which limits the time-resolution severely.

The length scales that can be easily accessed by SR SAXS are roughly from 1 to 100 nm. The range that can be studied is less dependent on the optics of the beam line but mainly on the physical active area from the position sensitive detector that is available on the beam line.

It should be noted that the low angle resolution is often seen as the most important parameter of a beam line. However, we do not necessarily agree with this point of view. In several scattering vector regimes different information is hidden (see Fig. 1). Quite often the most interesting experiments are those in which the scattering can be detected over a large angular range [22] which, unfortunately is often difficult to achieve. In the first place due to the finite size of position sensitive detectors and in the second place due to the fact that the scattered intensity falls of rapidly in intensity as function of the scattering angle. In a time-resolved experiment, where the time-frame length is set to the relevant time scale imposed by the speed in which structures develop it is often difficult to obtain sufficiently high data quality in the intermediate scattering range (Porod range) to be able to derive accurate structural parameters. However, often it is clear that the data in this range varies systematically in time. With sufficient information of other techniques the SAXS data set can then be used to derive kinetic parameters. It should be stated here that often the combination of time-resolved scattering data with post-mortem obtained real space data from, for instance, transmission electron microscopy (TEM) can in the end can be used to unravel the full story regarding the structural developments and the kinetics of these.

The different scattering regimes indicated in Fig. 1 do not have rigid boundaries but these are particle size dependent. It should also be noted that for non-particulate scattering, like for instance lamellar or interpenetrating networks similar parameters could be derived. However, an extensive treatment of this is beyond the scope of this text.

To describe briefly some of the parameters that can be derived from a SAXS experiment we will limit ourselves to a model system of a carrier material. We hope that this will give the reader a flavour of the possibilities of SAXS since due to space restrictions we cannot comprehensively treat the many aspects of this technique here. The carrier material for a useable catalyst will be by nature porous like for instance a zeolitic material. The porosity of this material, like for instance a zeolitic material, can be to some degree determined in a SAXS experiment and therefore generate a high scattering intensity. The electron density difference between the matrix and the pores will be by definition high. The size of these pores will be 1 nm or larger. In this case the low angle scattering,

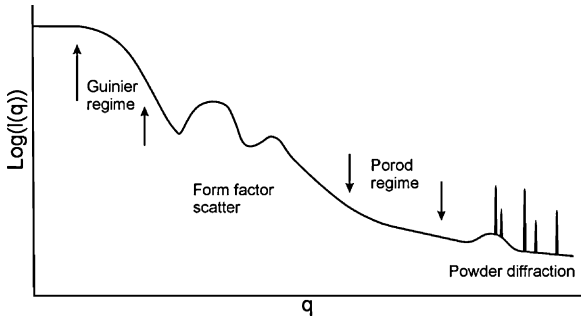

Fig. 1. Typical (stylised) SAXS/WAXS pattern in which the different scattering regimes are depicted. At the very lowest angles and can obtain information about large scale electron density fluctuations. The Guinier regime contains nformation about particle size and polydispersity. In the intermediate range one finds information about the particle shapes. The Porod regime contains information on the smoothness of interface layers and also about the total internal surface to volume ratio.

see Fig. 1, can be described by the so called Guinier law [23] which states that $I(q) \sim e^{-q^2 R_g/3}$. In this $I(q)$ is the scattered intensity, q the scattering vector and R_g the radius of gyration. This last parameter can be correlated with the real particle size if the shape of the pore is known [23]. In most cases one can assume a spherical symmetry in which case the real pore size can be correlated with the R_g via the relation $R = \sqrt{3/5}R_g$. The R_g can be determined from a plot of $I(q)$ vs q in the region where the condition $R_q q \ll 1$ is satisfied. A complication occurs when there is size polidispersity. In this case the data can be fitted by assuming that there is a Gaussian distribution of particle sizes [24]. This can render a rather good approximation to the pore size distribution although it should be remarked that a cross correlation with electron microscopy data will increase the reliability of the fitting procedure considerably.

In catalyitic materials the total internal surface is obviously of importance as well. The information on this is contained in the wider angle regime where the condition $R_q q \gg$ is met. Then the data can be approximated with the Porod equation [23] which states that $I(q)_{q\to\infty} \sim K_1 + K_2/q^4$ where K_1 is a q independent factor related to density fluctuations which for catalyst carriers can usually be ignored. K_2 is a parameter which contains the information on the total internal surface to volume ratio and will be discussed later. In the Porod approximation one assumes a sharp electron density variation between the pores and the carrier material. If this is not the case the equation has to be modified. Analytical approximations exist for a linear and sigmoidal density gradient [25]. The approximation for the most often occurring sigmoidal interface reads $I(q)_{q\to\infty} \sim K_1 + K_2 e^{-\sigma^2 q^2}/q^4$ in which σ is the half width of the sigmoid. The cases where a more irregular rough surface exists can be recognised by the fact that the exponent of -4 in the denominator does not render a reliable fit but is <4. It should be remarked here that the rather fast decay in the scattering intensity sometimes makes it difficult to obtain statistically reliable data in this scattering regime. This is especially the case in time-resolved data where the length of the time frames is decided by the speed with which the sample evolves. However, in general it is not difficult to determine the tendencies in the evolution of K_1, σ and the exponent thus providing information on the evolution of the system even though the exact parameters might have rather large error margins.

A rather accurate parameter that can be determined is the total scattering intensity which in the case of an isotropically scattering system is given by $Q = \int_0^\infty I(q) q^2 dq$. Historically this is unfortunately named the 'Invariant'. The unfortunate fact is that for a developing system this is rarely a non-changing parameter. In a two phase system it is correlated with the volume fractions $\phi_{1,2}$ of the two phases by $Q = \langle n_e \rangle^2 \phi_1 \phi_2$ in which n_e is the electron density difference between the two phases. If one of the two phases grows at the expense of the other phases or if the electron density difference changes it is obvious that the 'invariant' can vary in time. This can render important kinetic information, or alternatively, in combination with WAXS data, shed light on which phase crystallises in a phase separated system [26]. Since the determination of Q involves an integration over a large q-range all the pixels on a detector can be used which renders a high statistical accuracy.

When the invariant and the parameter K_2 have been determined one has the tools to determine the total internal surface to volume ratio via the relation $K_2/Q = 1/\pi S/V$. Obviously one has to be careful when using this relation since, as remarked before the statistical quality of the parameter K_2 might be low. However, tendencies in the development of the system can be observed and (post-mortem) cross correlation with electron microscopy, infrared spectroscopy or Raman scattering can increase the confidence level of the data.

Since the information content of SAXS data, without cross correlations with other information is rather low one occasionally finds alternative data analysis schemes in the literature [15]. These often involve the application of the concept of fractals to describe the morphology of the sample. The mass or surface fractal dimension of the sample can be correlated with growth processes and thus be used to distinguish between for instance reaction or diffusion limited kinetics in the growth process [27,28]. This is not a-priory wrong as long as one obeys certain rules. The fractal dimension can be determined from the slope of a straight section in a $^{10}\log I(q)$ vs. $^{10}\log q$ plot [14,15]. However, one should realise that this is only valid in the scattering vector regime where neither the Porod nor the Guinier equation are valid, i.e. in the intermediate scattering regime. An extra consideration here should be that true fractalline morphologies should extend over at least a decade of the scattering vector range. If this last condition is not satisfied one should avoid the fractal concept even if the data over a certain q range shows linear behaviour in a $^{10}\log I(q)$ vs. $^{10}\log q$ plot. Unfortunately one can find many examples in the literature where this last condition is ignored and a straight section over a fraction of a decade in q is used as evidence for the presence of fractal morphology. One should realise that already in Antique Greece it was known that two single data points define a straight line but that in modern times one should have the common sense to not over interpret data. A thorough description of how to handle data involving fractal morphology is given in [29,30].

In the case that catalytically active metal containing particles are embedded in a matrix the scattering of these particles can dominate the scattering of the matrix and one can apply the theory for single scatterers. This states that the scattering intensity is given by $I(q) = CS(q)|F(q)^2|$ where C is a constant related to the number of electrons in the scattering volume, $S(q)$ is the (liquid like) structure factor and $F(q)$ is the form factor. The structure factor details how the scattering intensities are dispersed in space and the form factor is dependent on the shape of the particle. The form factor of a spherical particle is given by $F(q) = [3(\sin qR - qR \cdot \cos qR)/(qR)^3]^2$. The mathematical expressions for many other particle shapes as well as several approaches for the structure factor are discussed in the review by Pedersen [31].

In real-time studies the importance of an appropriate sample environment that can impose the parameter, which one would like to vary in order to initiate the structural developments in the sample, is of paramount importance. These parameters can be temperature, (hydro-thermal) pressure or the chemical state of the sample. One should always take care that the parameter gradients over the sample are small enough with respect to the time resolution. When one for instance carries out a very rapid temperature quench which creates temperature gradient over the sample one should contemplate if a somewhat slower quench with fewer gradients would not render better insights into the process under consideration.

The capacity of the different techniques to detect structural changes is also something that one should be aware of. An example of this is that in a crystallisation process it is relatively simple to observe an increase in the total SAXS scattering intensity before one observes the evidence of structural changes in the sample on the crystalline level based upon the occurrence of crystalline peaks [15,32,33]. Since SAXS is sensitive to electron density variations, independent if the contrast is between an amorphous or crystalline particle compared to the matrix, it is a very sensitive probe to changes but not so much to the exact nature of these changes. In some cases the occurrence of an increase in SAXS intensity indicates that the small nano-particles that are formed start of amorphous only to become crystalline at a later stage. However, this interpretation is not always correct. The fact that no crystalline peaks are observed can also be due to the fact that small particles generate intrinsically broader diffraction peaks, the so-called Scherrer broadening. When the process takes place under elevated

temperatures there is also a temperature factor that tends to broaden the peaks. The combination of these two effects can, at the onset of crystallisation, broaden the diffraction peaks so much that the intensity becomes invisible in the statistical background intrinsic to every physical measurement. This can obscure the fact that these particles are crystalline from the onset. To resolve such questions one would require additional experimental techniques.

In the following section we describe some experiments that are illustrative for the way that X-ray scattering can be used to study the development of nanoporous materials.

Systems–Nanoporous materials: Nanoporous aluminosilicates and aluminophosphates and many other metal ions substituted variants are a part of the family of zeotype materials whose intricate pores and channels are in the size range of 0.3–2 nm, and have widely been used in a variety of applicaions which include catalysis, adsorbents and ion-exchangers [34–36]. Preparation of these novel nanoporous materials are at present an important field of research, in particular towards the production of materials with new pore structures. Several studies have been directed towards the understanding of the mechanism involved in the production of microporous materials [32,33,37–45]. Despite the continued efforts in understading the formation of these zeotype solids, due to the complexity of the formation process, its mechanism is not completely understood and it has been recognised that it is necessary to understand the crystallisation mechanism in detail to synthesize nanoporous mateials by rational design. Several attempts have been made in the past to unravel the complex mechanism of the zeolite formation, both computationally [46–49] and experimentally [32,33,37–45,50–53] employing both *in situ* and *ex situ* methods. For example SAXS and combined SAXS/WAXS techniques were extensively used with the aim to understand the nucleation and crystallisation processes that takes place during the formation of open framework structures [13,39,40,54–60]. Mintova et al studied the synthesis of nanosized aluminosilicate LTA and FAU structures from a colloidal solution and showed the steps of the generation and the densification of precursor particles to nanosized open framework materials by high resolution transmission electron microscopy (HRTEM) [61–64]. More recently, we reported the study of formation of zeolite A from clear solution and the study showed that, depending on the content of sodium hydroxide, 5 nm particles were observed to form prior to the crystallisation of zeolite A [32,33,41,65].

Another system of considerable interest is the formation of microporous aluminophosphate materials. Both large pore AlPO-5 (IZA code AFI) and small pore AlPO-34 (IZA code CHA) based systems were extensively studied due to their potential applications in catalysis [66–71]. In particular the understanding of the synthesis of large pore, AFI structured materials of considerable interest, since they are known to process large organic molecules. Recently we showed that 1 percent iron susbtituted AlPO-5 material can efficiently convert benzene molecules to phenol in the presence of nitrous oxide [69,70]. Earlier studies using energy dispersive X-ray diffraction methods clearly showed that, in the presence of cobalt ions, small pore materials, either AlPO-18 or AlPO-34 are formed [72–74] unless the pH of the starting gel is maintained around 6. Thus it is of considerable interest to

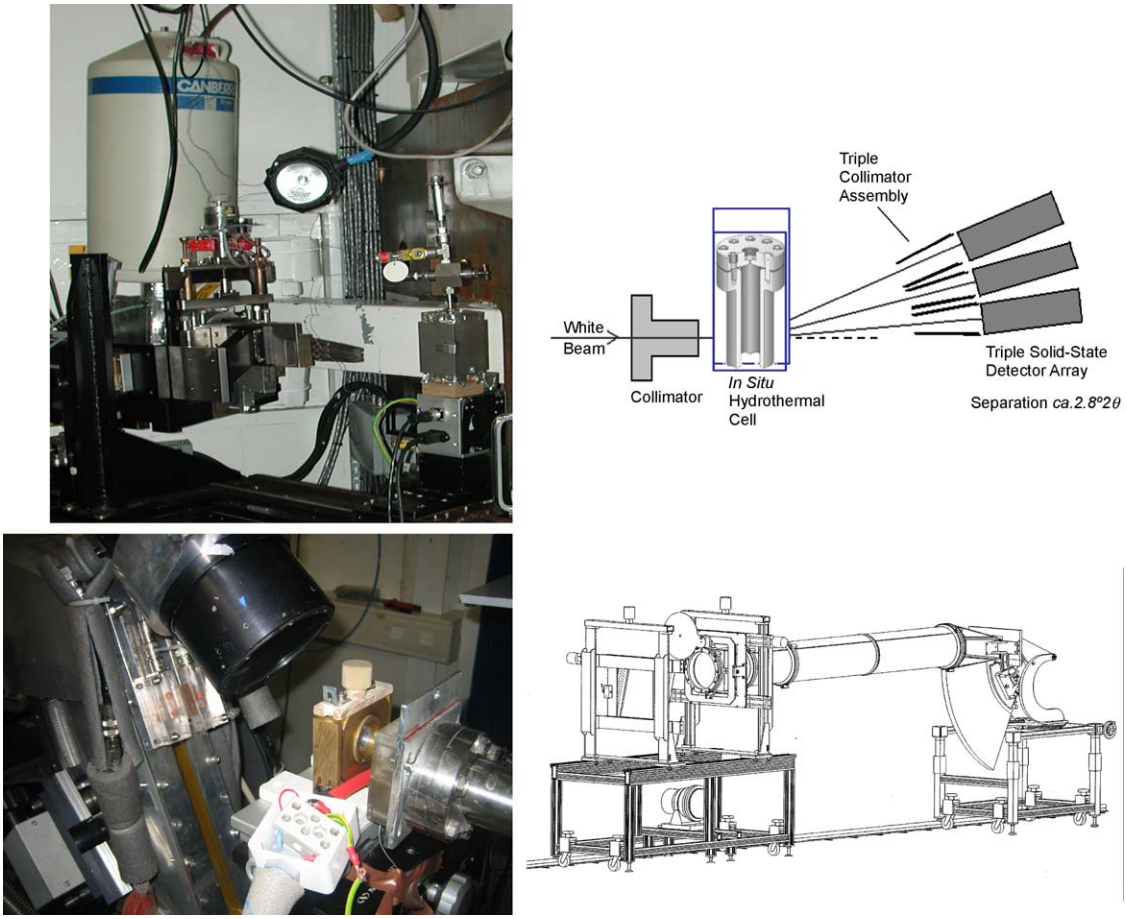

Fig. 2. EDXRD (top) and SAXS/WAXS (bottom) setup is shown here with a schematic diagram of the setup on the right side. In the top photograph, X—energy dispersive XRD detector and Y oven containing hydrothermal reaction vessel, are indicated. In the bottom photograph. (A) Hydrothermal cell used for SAXS/WAXS study, (B) vaccum chamber leading to the SAXS detector and (C) XRD detector, are shown.

investigate the formation of the large pore AFI material in the presence of transition metal ions, in particular the changes that take place prior to the formation of crystalline material.

Here, we review some of our time-resolved *in situ* study of the nucleation and crystal growth of nanoporous zeolite A and CoAlPO-5 systems using the combined SAXS/WAXS and energy dispersive X-ray diffraction (EDXRD) techniques.

2. Experimental

Typical gel mixtures used for the preparation of zeolitic solids are reported elsewhere [33,74]. In a typical *in situ* study, the solution containing appropriate amounts (molar ratio) of the respective ingredients were introduced into a specially designed *in situ* cell. This *in situ* cell was placed in an electrically pre-heated (to a specific temperature) oven. *In situ* SAXS/WAXS measurements were started as soon as the cell containing the gel was introduced and they were performed at BM26B, DUBBLE of the synchrotron radiation source at ESRF, France. A sample to detector distance of 8.0 m and 1.3 m, in order to cover different scattering vector ranges, were used in this work and the data were recorded using a wavelength of 1.4 Å. High-quality SAXS and WAXS patterns were collected simultaneously at every 2 min. The scattering from water was subtracted as the background. The scattering pattern of a standard sample (wet rat tail collagen) and the diffraction pattern of NaA zeolite were used to calibrate the patterns of SAXS and WAXS, respectively. SAXS data were analysed using the XOTOKO program available at Daresbury laboratory. EDXRD patterns were recorded at station 16.4 of Daresbury laboratory. In a typical experiment, the reaction mixture was introduced into a stainless steel autoclave and it was placed inside the oven just prior to the start of the measurements. EDXRD patterns were recorded every 2 min during the hydrothermal reaction [72,73]. Typical experimental arrangements of EDXRD and SAXS/WAXS techniques are shown in Fig. 2.

3. Results and discussion

First we discuss the energy dispersive X-ray diffraction data recorded during the crystallisation of zeolite A followed by the results of SAXS and WAXS data and then discuss the results of crystallisation of CoAlPO-5 material.

3.1. Zeolite A

In Fig. 3(a) we show a structural model of zeolite A and in (b) we show a typical EDXRD pattern recorded during the crystallisation of zeolite A, at 100 °C. A structure less, broad hump (circled in Fig. 3) appears during the initial stages of the crystallisation, which suggests that a non-crystalline material formed prior to the formation of crystalline solids. After several minutes of hydrothermal reaction, diffraction peaks appear and all the reflections seem to grow at similar rate indicating an uniform growth. The synthesis was performed at different temperatures and the change in the area under the (2 2 0) reflection with time is plotted in Fig. 3(c). It is clear from this figure that depending on the temperature, the start of the crystallisation process changes, which we term as induction time. It is observed that the higher the temperature shorter the induction time for a given chemical composition. We also plotted the full width at half maximum

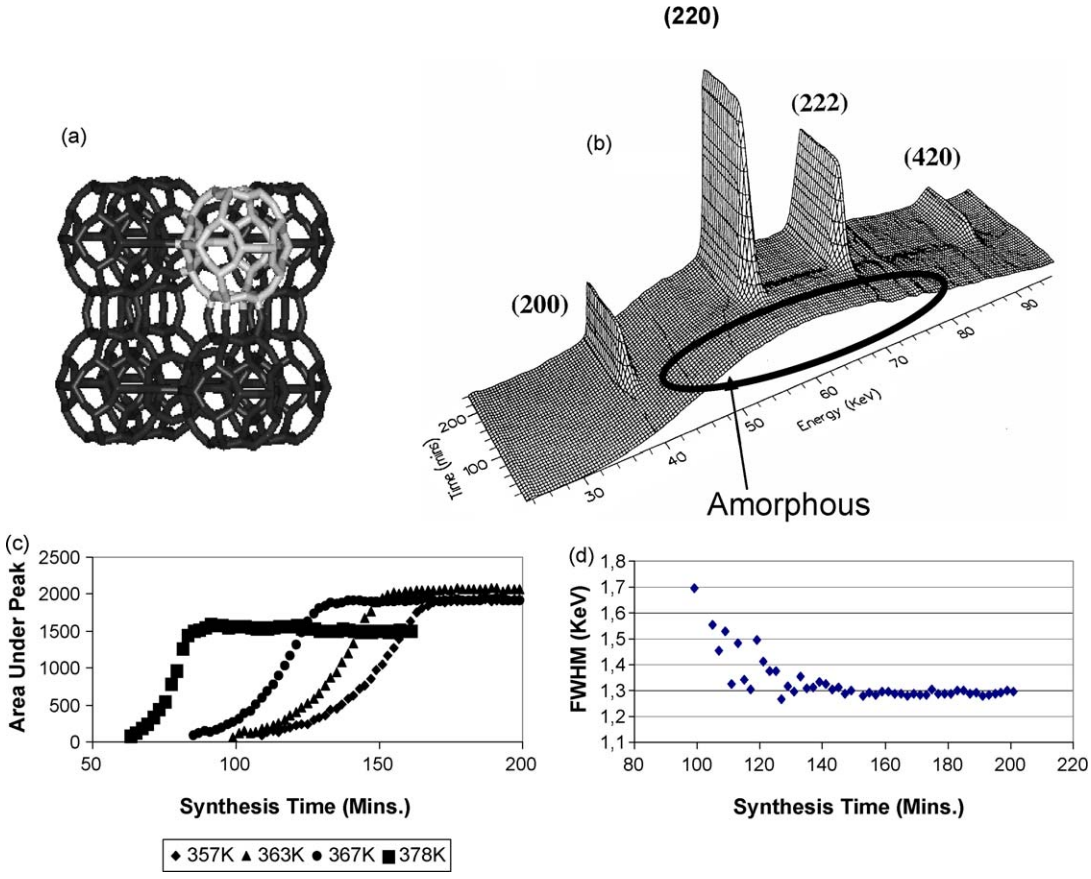

Fig. 3. A typical zeolite A structure is shown in (a); the sodalite cage is highlighted here. In (b) we show a typical EDXRD pattern of zeolite A, recorded during the hydrothermal synthesis at 100 °C. In (c) we show the variation of the area of the peaks corresponding to (2 0 0), (2 2 0), (2 2 2) and (4 2 0) reflections, with time, which suggests a uniform growth. The variation in the full width at half maximum (FWHM) of the (2 2 0) reflection with time is shown in (d).

(FWHM) obtained from the line-profile fitting of (2 2 0) reflection, for a given temperature, with time to determine the variation in particle size during the growth process (see Fig. 3(d)). As one would expect, the decrease in FWHM from *ca.* 1.7–1.3 keV suggest that particles are small at the initial stages and grows for about 20 min after the initiation of the crystallisation processes and remain unaltered after 120 min of the hydrothermal reaction. Although the information derived from EDXRD technique enabled us to determine the kinetics of crystallisation and activation energy of the process it was not possible to determine the nature of particles formed just prior to the crystallisation of zeolite A, in particular for the amorphous material. Hence we investigated this system, in detail, using SAXS/WAXS technique.

Time-resolved stacked WAXS and SAXS patterns are shown in Fig. 4(a) and (b), respectively. (The SAXS data shown here are processed to remove the background by subtracting the SAXS pattern of water, similar to the method followed by deMoor et al. [13]); this data was recorded using a sample-detector distance of *ca.* 8 m. It is clear from Fig. 4(b), a broad hump appears in the SAXS pattern after heating the clear solution for about 16 min. This hump spreads over a Q range of *ca.* 0.7 and 0.4 nm^{-1} which corresponds to *ca.* 5 and 15 nm with centre of the hump at *ca.* 10 nm (calculated using the equation $d = 2\pi/Q$, where Q is $4\pi \sin(\theta)/\lambda$) [13,39,40,56] . The position of the maximum point of the hump moves to a lower Q value with time; the hump centred around *ca.* $Q = 0.79$ nm^{-1} ($d = 8$ nm), measured after 16 min of the reaction moves to *ca.* $Q = 0.48$ nm^{-1} ($d = 13$ nm) at 32 min. Particle size estimated from the position of the broad hump clearly shows that it has increased from 8 nm to 13 nm over a period of 16 min. WAXS patterns recorded simultaneously during the SAXS measurements did not show any Bragg reflections, indicating that the crystallization has not taken place, which is similar to the one observed by EDXRD data. After 42 min of the hydrothermal reaction, although the intensity of the broad hump appears to have decreased slightly, its position ($Q = 0.44$ nm^{-1} ($d = 15$ nm)) remained closely similar to the earlier observation made at *ca.* 32 min, suggesting that the particle size has not signifcantly changed. More interestingly, an oscillatory pattern appears in the low Q region of the SAXS patterns recorded after 32 min, which also coincides with the appearance of reflections in the WAXS pattern. We fitted this oscillatory part of the data assuming a cubic morphology (confirmed through SEM measurements) and determined the particle size of the material formed during the crystallisation process. In Fig. 4(c) we plotted the variation in particle size with time measured at different temperatures. It is clear from this plot that at higher synthesis temperatures larger particles are formed suggesting a growth dominating process at higher temperatures.

We also carried out a series of experiments using a short sample to detector distance (1.3 m) thus changing the scattering vector range that can be observed. The advantage with the short sample detector distance is that, the q-range is in such a way that both SAXS pattern and part of the Bragg scattering can be observed with the same detector. Typical stacked plot, recorded during the crystallisation of zeolite A from a clear solution is shown in Fig. 4(d). Here we can see clearly several changes in the small angle region, in parituclar formation of a broad hump similar to the one observed using a long sample to detector distance, described above. A Bragg peak related to crystalline zeolite A starts to appear at high q region (marked as X in Fig. 4(d)) after about 35 min of crystallisation. Thus the combination of two sample-detector distances not only provide a wide q-range to extract information

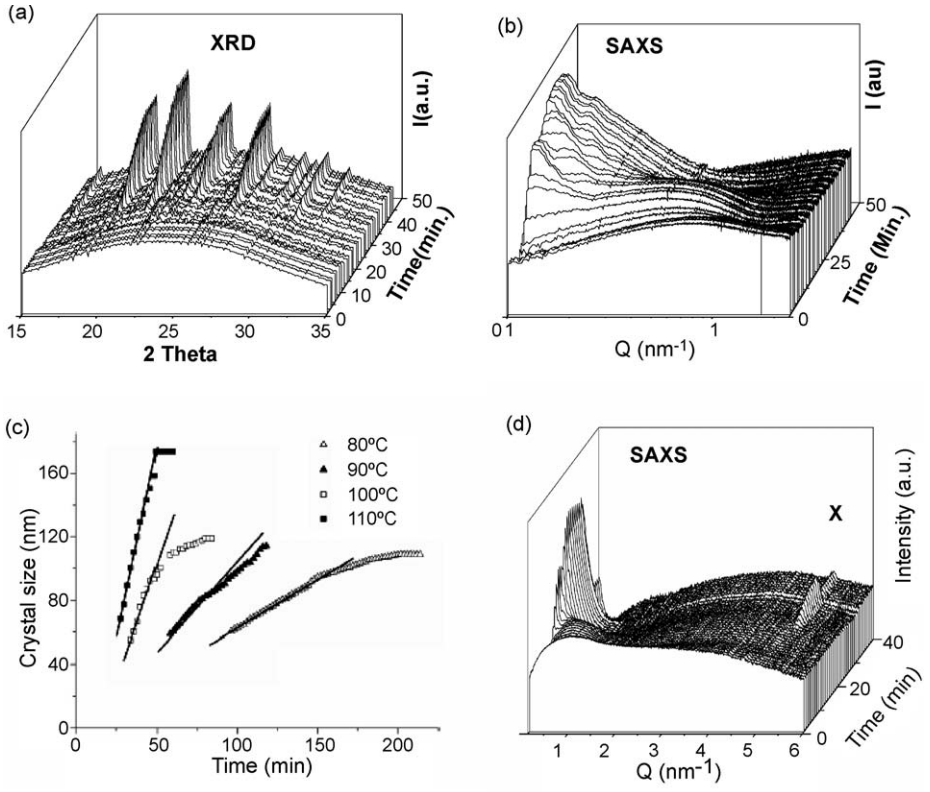

Fig. 4. *In situ* time-resolved WAXS in (a), SAXS in (b), recorded during the hydrothermal synthesis of zeolite A, at 100 °C, are shown here along with the variation in particle size, estimated from the broad hump in (b), with time is shown in (c). In (d) we show the time-resolved SAXS pattern recorded during the hydrothermal crystallisation of zeolilte A measured using a short (1.3 m) sample-detector distance. X indicates the Bragg reflection arising from the crystals of zeolite A. (To emphasize the details in the scattering pattern the data is plotted as $I(q)q^2$. This is only for display purposes and no physical relevance should be attributed to this.)

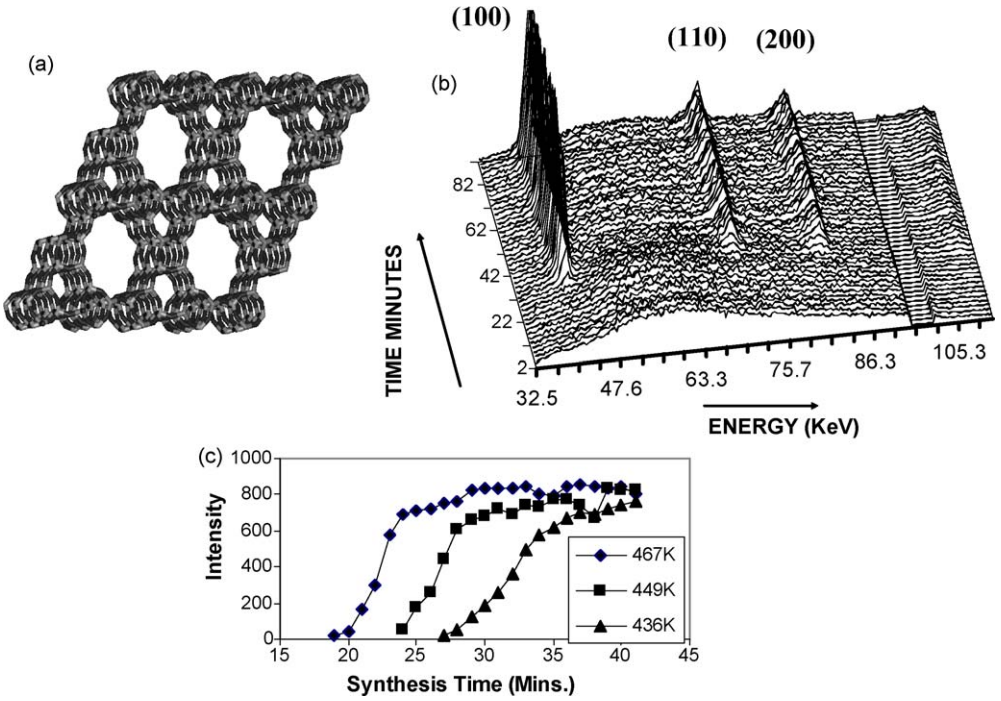

Fig. 5. Structure of AlPO-5 (AFI, International Zeolite Association code) is shown in (a). A typical time-resolved EDXRD data recorded during hydrothermal reaction of a CoAlPO-5 gel, at 160 °C is shown in figure (b). In (c) we show the variation in the area under the peak of reflection (1 0 0), with time, recorded at three different temperatures.

prior to the crystallisation processes, but also, in some cases provide simultaneous information on the formation of crystalline solid during the hydrothermal process.

3.2. CoAlPO-5

Typical structure of the large pore AFI is shown in Fig. 5(a) and the EDXRD pattern recorded, *in situ*, during the crystallisation of CoAlPO-5 (Co content was 4% and the pH of the starting gel was maintained at 6 pH and the synthesis temperature is *ca.* 165 °C) is shown in Fig. 5(b). The first reflection was analysed by fitting the peak and the area under the curved determined is plotted against time in Fig. 5(c). The EDXRD pattern shown in Fig. 5(b) shows a structure less pattern in the data recorded during the initial stages of the hydrothermal reaction and after *ca.* 20 min the reflections respesenting pure AFI phase starts to appear in the EDXRD

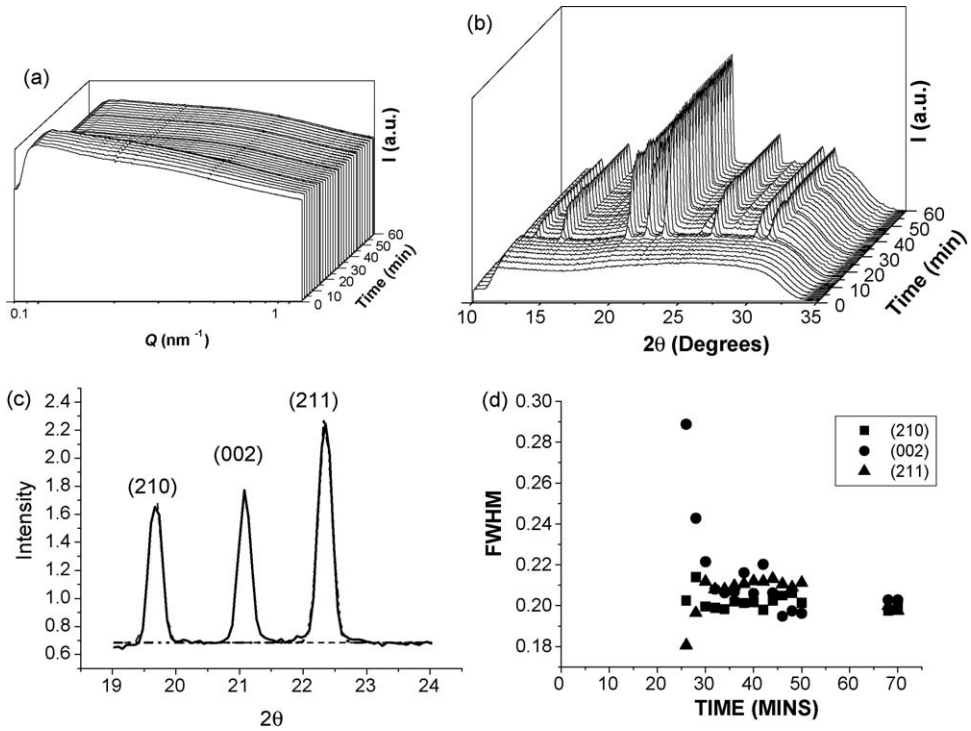

Fig. 6. The time-resolved SAXS (in (a)) and WAXS (in (b)), recorded during the formation of CoAlPO-5, under hydrothermal conditions at *ca.* 160 °C, are shown here. In (c) we show a typical fit to the three reflections appears between 19 and 24 2θ. In (d) we show the variation in the full-width at half maximum for the three reflections, obtained from the best fit, with time.

patterns. Plot of the area under the (1 0 0) reflection with time, shown in Fig. 5(c) indicates the growth of the CoAlPO-5 material during the hdyrothermal reaction. Hydrothermal reactions conducted at various temperature (see the growth curve obtained from reactions conducted at three different temperatures in Fig. 5(c)) shows that at higher temperatures not only the reaction proceeds faster, but also the induction period is decreased to a lower value, typically seen for the kinetically driven processes. Earlier studies [74] using combined XRD/XAS (at the Co K-edge) revealed that the Co(II) ions present in octahedral coordination are converted to tetrahedral coordination just prior to the crystallisation of CoAlPO-5 material.

We performed the *in situ* SAXS/WAXS studies of the crystallisation of microporous aluminophosphate, using a gel mixture similar to the one used for EDXRD and combined XRD/XAS studies and the stacked plot of the SAXS and WAXS patterns are shown in Fig. 6. The SAXS pattern in Fig. 6(a) did not show well-defined characteristics as seen for zeolite A. Although the SAXS data (see Fig. 6(a)) appears to be featureless, we utilised the change in slope of the SAXS pattern of the data recorded simulataneously when the WAXS patterns showed indications of the appearance of the reflections corresponding to AFI structure and the particle size estimated from the analysis indicate that about 50 nm particles are formed just prior to the crystallisation of AlPO-5 structure [17,75]. The WAXS data (see Fig. 6(b)) clearly showed the presence of only phase pure AlPO-5 [74] material under the reactions conditions used in this work. Further information can also be gained from the WAXS data. In particular, we analysed the three reflections, (2 1 0), (0 0 2) and (2 1 1) (see Fig. 6(c)) and found that the variation in the full-width at half maximum (FWHM) (indicativeof the particle size) does not vary at the same rate in all the cases (see Fig. 6(d)). FWHM of the (0 0 2) reflection, in particular, showed a slow decrease indicating that the particles were much smaller in the c-direction at the initial stages and they grow during the crystallisation process. A more detailed study is in progress to address this issue and gain further insight into the mechanism of formation of AlPO-5 structure.

In summary, the *in situ* SAXS/WAXS investigation, indicate the formation of zeolite A precursors with a particle size in the range of *ca.* 10 nm before the onset of crystallisation. The occurrence of oscillations in the low Q region of the SAXS data suggest that a homogeneous nucleation leading to LTA crystals with narrow size distribution are formed under these synthesis conditions. However, similar such homogeneous crystallisation is not observed for the formation of the CoAlPO-5 system.

4. Conclusions

We have given a brief overview of the possibilities and limitations that technique combinations based upon X-ray scattering can provide for researchers in the field of catalysis especially in systems where one wants to study the evolution of morphology or determine kinetic parameters. The examples shown here are not exhaustive in showing what is feasible. For instance we have not addressed the issues of how to obtain kinetic parameters from either the SAXS or WAXS data. This is mainly due to space limitations.

The intelligent use of X-ray scattering techniques can render beautiful insights in many aspects of systems that are relevant in catalysis research. This can range from kinetic parameters to morphological issues. So far the full potential of this type of work has not been utilised yet. This is partly due to the lack of the required infrastructure on existing beam-lines with respect to the appropriate detectors and sample environments. However, this research is also hampered by the lack of a sufficient number of beam lines that can provide the volume of beam-time that is required.

Acknowledgments

GS thanks Royal Society for UK-Japan visiting fellowship. GS also thanks CLRC, Daresbury laboratory for provision of beam time and facilities and Dr C. Martin and Dr D. Taylor for useful discussions. The DUBBLE staff are also acknowledged for their assistance. Acces to the BM26B DUBBLE beamline at the ESRF was provided by the Dutch and Flemish research councils (NWO-FWO).

References

[1] C.R.A.C.a.G.N. Greaves, Applications of Synchrotron Radiation, Springer, 1990.
[2] J.W. Niemantsverdriet, Spectroscopy in Catalysis, Wiley–VCH, Amsterdam, 2000.
[3] B.S. Clausen, L. Grabaek, G. Steffensen, P.L. Hansen, H. Topsoe, Symposium on X-Ray Absorption Fine Structure: Catalysts and Related Surfaces, Tokyo, Japan, August 31–September 1, 1992.
[4] B.S. Clausen, H. Topsoe, R. Frahm, Advances in Catalysis 42 (1998) 315.
[5] J.W. Couves, J.M. Thomas, D. Waller, R.H. Jones, A.J. Dent, G.E. Derbyshire, G.N. Greaves, Nature 354 (1991) 465.
[6] G. Sankar, J.M. Thomas, D. Waller, J.W. Couves, C.R.A. Catlow, G.N. Greaves, Journal of Physical Chemistry 96 (1992) 7485.
[7] G. Sankar, J.M. Thomas, Topics in Catalysis 8 (1999) 1.
[8] G. Sankar, J.M. Thomas, C.R.A. Catlow, Topics in Catalysis 10 (2000) 255.
[9] K. Iino, M. Anpo, Research on Chemical Intermediates 29 (2003) 773.
[10] W. Bras, 3rd International Conference on Synchrotron Radiation in Materials Science, Singapore, Singapore, January 21–24, 2002.
[11] W. Bras, I.P. Dolbnya, D. Detollenaere, R. van Tol, M. Malfois, G.N. Greaves, A.J. Ryan, E. Heeley, 12th International Conference on Small-Angle Scattering, Venice, Italy, August 25–29, 2002.
[12] T.P.M. Beelen, W.H. Dokter, H.F. Vangarderen, R.A. Vansanten, E. Pantos, IX International Conference on Small Angle Scattering, Saclay, France, April 27–30, 1993.
[13] P. deMoor, T.P.M. Beelen, R.A. vanSanten, Microporous Materials 9 (1997) 117.
[14] W.H. Dokter, T.P.M. Beelen, H.F. Vangarderen, R.A. Vansanten, W. Bras, G.E. Derbyshire, G.R. Mant, Journal of Applied Crystallography 27 (1994) 901.
[15] W.H. Dokter, H.F. Vangarderen, T.P.M. Beelen, R.A. Vansanten, W. Bras, Angewandte Chemie-International Edition in English 34 (1995) 73.
[16] W. Bras, A.J. Ryan, Advances in Colloid and Interface Science 75 (1998) 1.
[17] A.M. Beale, A.M.J. van der Eerden, S.D.M. Jacques, O. Leynaud, M.G. O'Brien, F. Meneau, S. Nikitenko, W. Bras, B.M. Weckhuysen, Journal of the American Chemical Society 128 (2006) 12386.
[18] J.G. Mesu, A.M.J. van der Eerden, F.M.F. de Groot, B.M. Weckhuysen, Journal of Physical Chemistry B 109 (2005) 4042.
[19] M.H.J. koch, W. Bras, Annual Reports on the Progress of Chemistry Section C 104 (2008) 35.
[20] W. Bras, S.M. Clark, G.N. Greaves, M. Kunz, W. van Beek, V. Radmilovic, Crystal Growth & Design 9 (2009) 1297.
[21] J.C. Mauro, S.S. Uzun, W. Bras, S. Sen, Physical Review Letters 102 (2009).
[22] W. Bras, G.N. Greaves, M. Oversluizen, S.M. Clark, G. Eeckhaut, Journal of Non-Crystalline Solids 351 (2005) 2178.
[23] O. Glatter, O. Kratky, Small Angle X-ray Scattering, Academic Press, 1982.
[24] J. BrunnerPopela, O. Glatter, Journal of Applied Crystallography 30 (1997) 431.
[25] J.T. Koberstein, B. Morra, R.S. Stein, Journal of Applied Crystallography 13 (1980) 34.
[26] S. Nikitenko, A.M. Beale, A.M.J. van der Eerden, S.D.M. Jacques, O. Leynaud, M.G. O'Brien, D. Detollenaere, R. Kaptein, B.M. Weckhuysen, W. Bras, Journal of Synchrotron Radiation 15 (2008) 632.
[27] H.D. Bale, P.W. Schmidt, Physical Review Letters 53 (1984) 596.
[28] P.W. Schmidt, 8th International Conference on Small Angle Scattering, Louvain, Belgium, August 6–9, 1990.
[29] G. Beaucage, D.W. Schaefer, 2nd International Discussion Meeting on Relaxations in Complex Systems, Alicante, Spain, June 28–July 8, 1993.
[30] J.E. Martin, A.J. Hurd, Journal of Applied Crystallography 20 (1987) 61.
[31] J.S. Pedersen 3rd, European Summer School on Scattering Methods Applied to Soft Condensed Matter, Bombannes, France, 1997.
[32] W. Fan, F. Meneau, W. Bras, M. Ogura, G. Sankar, T. Okubo, International Symposium on Zeolite and Microporous Crystals (ZMPC 2006), Yonago, Japan, July 30–August 2, 2006.
[33] W. Fan, M. O'Brien, M. Ogura, M. Sanchez-Sanchez, C. Martin, F. Meneau, K. Kurumada, G. Sankar, T. Okubo, Physical Chemistry Chemical Physics 8 (2006) 1335.
[34] R.M. Barrer, Hydrothermal Chemistry of Zeolites, Academic Press, London, 1982.
[35] R. Szostak, Molecular Sieves, Blackie, 1997.
[36] P.A. Wright, Microporous Framework Solids, RSC Publishing, Cambridge, 2007.
[37] C.S. Cundy, P.A. Cox, Chemical Reviews 103 (2003) 663.
[38] C.S. Cundy, P.A. Cox, Microporous and Mesoporous Materials 82 (2005) 1.
[39] P. de Moor, T.P.M. Beelen, R.A. van Santen, L.W. Beck, M.E. Davis, Journal of Physical Chemistry B 104 (2000) 7600.
[40] P. de Moor, T.P.M. Beelen, R.A. van Santen, K. Tsuji, M.E. Davis, Chemistry of Materials 11 (1999) 36.
[41] W. Fan, M. Ogura, G. Sankar, T. Okubo, Chemistry of Materials 19 (2007) 1906.
[42] S.A. Pelster, R. Kalamajka, W. Schrader, F. Schuth, Angewandte Chemie-International Edition 46 (2007) 2299.

[43] F. Schuth, Current Opinion in Solid State & Materials Science 5 (2001) 389.
[44] F. Schuth, P. Bussian, P. Agren, S. Schunk, M. Linden, Meeting on Aspects of Modern Inorganic Chemistry: Nucleation, Self Assembly, Biomineralization and Crystal Growth, Paris, France, November 2000.
[45] D.P. Serrano, R. van Grieken, Journal of Materials Chemistry 11 (2001) 2391.
[46] M.J. Mora-Fonz, C.R.A. Catlow, D.W. Lewis, Angewandte Chemie-International Edition 44 (2005) 3082.
[47] M.J. Mora-Fonz, C.R.A. Catlow, D.W. Lewis, Journal of Physical Chemistry C 111 (2007) 18155.
[48] M.J. Mora-Fonz, S. Hamad, C.R.A. Catlow, 3rd International Conference on Foundations of Molecular Modeling and Simulation (FOMMS), Blaine, WA, July 9–14, 2006.
[49] S.A. Ojo, L. Whitmore, B. Slater, C.R.A. Catlow, Meeting on Aspects of Modern Inorganic Chemistry: Nucleation, Self Assembly, Biomineralization and Crystal Growth, Paris, France, November 2000.
[50] P. Norby, A.N. Christensen, J.C. Hanson, 10th International Zeolite Conference, Garmisch Partenkir, Germany, July 17–22, 1994.
[51] P. Norby, J.C. Hanson, 11th International Congress on Catalysis, Baltimore, MD, June 29–July 5, 1996.
[52] B. Panzarella, G. Tompsett, W.C. Conner, K. Jones, Chemphyschem 8 (2007) 357.
[53] G.A. Tompsett, B. Panzarella, W.C. Conner, K.S. Yngvesson, F. Lu, S.L. Suib, K.W. Jones, S. Bennett, Review of Scientific Instruments 77 (2006).
[54] C.H. Cheng, G. Juttu, S.F. Mitchell, D.F. Shantz, Journal of Physical Chemistry B 110 (2006) 22488.
[55] C.H. Cheng, D.F. Shantz, Journal of Physical Chemistry B 109 (2005) 13912.
[56] P. de Moor, T.P.M. Beelen, B.U. Komanschek, L.W. Beck, P. Wagner, M.E. Davis, R.A. van Santen, Chemistry—A European Journal 5 (1999) 2083.
[57] B.U. Komanschek, P. de Moor, T.P.M. Beelen, R.A. van Santen, 2nd International Conference on Synchrotron Radiation in Materials Science (SRMS-2), Kobe, Japan, October 31–November 3, 1998.
[58] M. Smaihi, O. Barida, V. Valtchev, European Journal of Inorganic Chemistry (2003) 4370.
[59] S.Y. Yang, A. Navrotsky, Chemistry of Materials 16 (2004) 3682.
[60] S.Y. Yang, A. Navrotsky, D.J. Wesolowski, J.A. Pople, Chemistry of Materials 16 (2004) 210.
[61] O. Larlus, S. Mintova, T. Bein, Microporous and Mesoporous Materials 96 (2006) 405.
[62] S. Mintova, N.H. Olson, T. Bein, Angewandte Chemie-International Edition 38 (1999) 3201.
[63] S. Mintova, N.H. Olson, J. Senker, T. Bein, Angewandte Chemie-International Edition 41 (2002) 2558.
[64] S. Mintova, N.H. Olson, V. Valtchev, T. Bein, Science 283 (1999) 958.
[65] G. Sankar, T. Okubo, W. Fan, F. Meneau, Faraday Discussions 136 (2007) 157.
[66] K. Mathisen, D.G. Nicholson, A.M. Beale, M. Sanchez-Sanchez, G. Sankar, W. Bras, S. Nikitenko, Journal of Physical Chemistry C 111 (2007) 3130.
[67] R. Raja, G. Sankar, J.M. Thomas, Journal of the American Chemical Society 121 (1999) 11926.
[68] G. Sankar, R. Raja, J.M. Thomas, Catalysis Letters 55 (1998) 15.
[69] G. Sankar, N.R. Shiju, I.D. Watts, S. Nikitenko, W. Bras, International Symposium on Design of Advanced Materials Using Nano Space, Osaka, Japan, August 4, 2006.
[70] N.R. Shiju, S. Fiddy, O. Sonntag, M. Stockenhuber, G. Sankar, Chemical Communications (2006) 4955.
[71] J.M. Thomas, R. Raja, G. Sankar, R.G. Bell, Accounts of Chemical Research 34 (2001) 191.
[72] A.T. Davies, G. Sankar, C.R.A. Catlow, S.M. Clark, Journal of Physical Chemistry B 101 (1997) 10115.
[73] F. Rey, G. Sankar, J.M. Thomas, P.A. Barrett, D.W. Lewis, C.R.A. Catlow, S.M. Clark, G.N. Greaves, Chemistry of Materials 7 (1995) 1435.
[74] G. Sankar, J.M. Thomas, F. Rey, G.N. Greaves, Journal of the Chemical Society—Chemical Communications (1995) 2549.
[75] D. Grandjean, A.M. Beale, A.V. Petukhov, B.M. Weckhuysen, Journal of the American Chemical Society 127 (2005) 14454.